compared with E^{-6}). This result is in accord with the theoretical intuition on which the BK calculation is based.

The relation of these results to experiment is uncertain at the present time, and further experiments on proton-hydrogen charge exchange are urgently required. If one believes that the charge-exchange cross sections determined from studies of proton-hydrogen molecule interactions are accurate and are representative of the cross section in proton-hydrogen atom scattering, the present results are unsatisfactorily large.[4,5] The situation is not better if Drisko's result based on higher Born approximations is used; for in that case the theoretical prediction is much too small at the energies for which the observations were made. We intend to attempt further investigations of higher-order terms in the Faddeev expansion for the transition amplitude [Eq. (2.3)] in order to determine whether there are any further corrections to σ of significance in the high-energy limit.

†Supported in part by the U.S. Office of Naval Research.

[1]L. D. Faddeev, Zh. Eksperim. i Teor. Fiz. 39, 1459 (1960) [English transl.: Soviet Phys. – JETP 12, 1014 (1961)].

[2]J. Schwinger, J. Math. Phys. 5, 1606 (1964).

[3]G. L. Nutt, J. Math. Phys. 9, 796 (1968).

[4]B. H. Bransden, Adv. At. Mol. Phys. 1, 85 (1965).

[5]B. H. Bransden, in Lectures in Theoretical Physics, edited by S. Geltman, K. T. Mahanthappa, and W. E. Brittin (Gordon and Breach, Science Publishers, Inc., New York, 1969, Vol. XIII-C, p. 139.

[6]H. C. Brinkmann and H. A. Kramers, Proc. Acad. Sci. Amsterdam 33, 973 (1930).

[7]J. C. Jackson and H. Schiff, Phys. Rev. 89, 359 (1953).

[8]R. M. Drisko, thesis, Carnegie Institute of Technology, 1955 (unpublished); R. McCarrol and A. Salin, Proc. Roy. Soc. (London) A300, 202 (1967); C. Pradham, and D. N. Tripathy, Phys. Rev. 130, 2317 (1963); also see Ref. 4.

[9]R. Aaron, R. D. Amado, and B. W. Lee, Phys. Rev. 121, 319 (1961).

[10]K. Dettmann and G. Leibfried, Z. Physik 210, 43 (1968).

[11]I. H. Sloan and E. J. Moore, J. Phys. B 1, 414 (1968).

[12]J. S. Ball, J. C. Y. Chen, and D. Y. Wong, Phys. Rev. 173, 2021 (1968).

[13]J. C. Y. Chen, K. T. Chung, and P. J. Kramer, Phys. Rev. 184, 64 (1969).

PHYSICAL REVIEW A VOLUME 1, NUMBER 4 APRIL 1970

Theoretical Calculation of Pressure-Broadened Atomic Line Profiles*

Makoto Takeo†

Department of Physics, Portland State University, Portland, Oregon 97207

and

Department of Physics, University of Oregon, Eugene, Oregon 97403

(Received 11 August 1969)

An atomic line profile is theoretically calculated for various relative densities at two temperatures (666 and 800 °K) under an adiabatic assumption, with a Lennard-Jones potential, and is compared with the experimental profile of the shorter-wavelength component of the resonance lines of cesium perturbed by xenon. The calculation predicts an appearance of one red satellite and two violet satellites as experimentally observed. Further, the result shows that the agreement between the pressure behavior of the theoretical line shape and that of the observed one is only qualitative, because the calculated satellite intensities are too weak. This disagreement is attributed to an inadequacy of the Lennard-Jones potential for calculating line-shapes under the present approximations.

INTRODUCTION

Recent experimental investigations on atomic line shapes perturbed by foreign gases in absorption[1] have revealed a complex behavior under various densities. There are various theoretical approaches for treating the problem,[2,3] but it is almost certain that the interatomic potential must be included to higher orders in the treatment even at low relative densities.[4] The simplest and most

commonly used approximation to the interatomic potential is a Lennard-Jones 6-12 potential.

Higher-order terms of the interaction potential must be included with the lowest one because of the following reason. In the impact approximation, strong collisions contribute to line broadening. Strong collisions occur with certain small impact parameters, where the phase shift is arbitrarily large (≥ 1). For a Cs-Xe pair, the van der Waals constant is 8.10^{-58} and 15.10^{-58} erg cm^6, respectively, when the Cs atom is in the ground state and the first excited $^2P_{1/2}$ state.[5] For this interaction, the impact parameter must be about 10 Å or less for a collision to be strong. For such short distances, the higher-order terms may become important.

In many cases, the atomic lines are isolated, but the energy levels associated with them are degenerate, and the adiabatic interatomic potential depends on the magnetic quantum number $|m|$. The repulsive part of the potential and its $|m|$ dependence are hard to evaluate. In addition, it is unlikely to be pairwise additive.

For the relative density (rd) range used in recent experimental observations,[1] the atomic mean distance is on the order of 10 or 20 Å. Therefore, many-body collisions are fairly common. Collisions are isotropic and random. As a result, the perturbation on the radiation process due to collision changes rather slowly in time and an adiabatic condition holds to a good approximation. However, this adiabaticity should not be confused with that in the rotating coordinate system with an isolated single colliding particle.[6] In the present case, the radiating atom finds nearby perturbers in almost all directions simultaneously. Thus, not only two-body forces but also exchange forces are nearly isotropic. The adiabaticity allows the radiating atom to remain in a definite state in a slowly fluctuating coordinate system with the total perturbation. Here, the total perturbation may be approximated by the sum of the effective interatomic potential per perturber which is obtained by averaging the $|m|$-dependent potential over m.

Thus, the line profile is calculated theoretically at two different temperatures (666 and 800 °K), under the adiabatic assumption, by introducing a Lennard-Jones potential as an effective potential for the pressure effect on the $^2P_{3/2}$ component of the cesium resonance lines perturbed by xenon [Cs(1)/Xe]. The difference in the upper and lower effective interatomic potential curves is estimated, in the form of a Lennard-Jones type, from Mahan's value[5] and the position of the red satellite.[3] This difference potential causes a smearing of the frequency emitted by the radiating atom due to the atomic relative motion. The path of the motion is assumed to be classical and straight. For high rd, this assumption is doubtful, but will not introduce a large error in the result since, in this case, the correlation function for small time is important. Under these experimental conditions, Doppler broadening can be ignored.

The result shows that there appear one red satellite and two violet satellites as the experimental observation,[7] but the calculated intensities are much too weak, suggesting that the effective Lennard-Jones potential is inadequate to account for the observed line shape.

It is noted that satellites discussed here are a part of the whole line, produced by the same mechanism as that for line broadening. Therefore, satellites lose their meaning if they overlap with the line unless they can be separated somehow under a definite rule.

We note that the logarithm of the autocorrelation function can always be separated into two parts, depending on large or small time, like Eqs. (6) and (7), analogous to the separation of the impact and the quasistatic approximation. The behavior of the effect of the two parts on the line shape at various pressures and temperatures is very different, as illustrated in Fig. 2. In this sense, the separation of the total intensity into the line and satellites is meaningful.

Now, Eq. (7), if its validity is extended to zero time, leads to the Anderson-Talman intensity profile.[8] Therefore, in the following we define the satellite as the difference between this profile and the total intensity contour. This definition of a satellite can also be applied to experimental observation by taking the Fourier transform of the total line contour, i.e., the autocorrelation function, and from this, finding the Anderson-Talman profile from the asymptote of the logarithm of this transform at large time.

THEORY

According to the correlation function approach, the line shape is given by the Fourier transform of the autocorrelation function,

$$\phi(\tau) = \langle M(\tau)M(0)\rangle \quad , \tag{1}$$

where $M(\tau)$ is the electric dipole moment of the entire absorbing system. The brackets indicate an averaging of the initial ensemble. Here the Boltzmann factor is ignored, because the mean in-

teraction energy is usually far less than the thermal energy.

If the adiabatic assumption holds, the correlation function can be written[3,8]

$$\phi(\tau)=e^{-N\psi(\tau)} \quad , \tag{2}$$

where N is the number density of the perturbers. If the interatomic potential difference, $\hbar V(R)$, is pairwise additive and the path of approach is classical and straight, we find that

$$\psi(\tau)=2\pi\int_0^\infty \rho d\rho \int_{-\infty}^{\infty} dy \times[1-\exp(-i\int_0^\tau V([\rho^2+(y+vt)^2]^{1/2}dt)] \quad . \tag{3}$$

The integral of Eq. (3) represents the average of Eq. (1) over the initial positions of perturbers. The velocity distribution is ignored for simplicity, and v is the mean relative velocity.

By performing an integration of Eq. (3), $\psi(\tau)$ can be found. But, for the purpose of relating the present calculation to the impact approximation, a large cut-off distance a_0 of the potential may be introduced. Then, Eq. (3) can be separated into two parts. Defining $\xi=v\tau$,

$$u=y+vt, \quad b=[a_0^2-(\xi^2/4)]^{1/2}, \quad \text{and} \quad c=(a_0^2-\rho^2)^{1/2}, \quad \text{for } \xi<2a_0 \quad ,$$

one obtains

$$\psi(\xi)=\psi_{\mathrm{I}}(\xi)+\psi_{\mathrm{II}}(\xi) \quad , \tag{4}$$

with

$$\psi_{\mathrm{I}}(\xi)=2\pi\xi\int_b^{a_0}\rho d\rho[1-\exp(-i\int_{-c}^{c}V\,[\rho^2+u^2]^{1/2})du/v)]+4\pi\int_b^{a_0}\rho d\rho\int_0^c dy[1+\exp(-\int_{-c}^{c}V([\rho^2+u^2]^{1/2})du/v) - \exp(-i\int_{-c}^{y}V([\rho^2+u^2]^{1/2})du/v)-\exp(-i\int_y^c V([\rho^2+u^2]^{1/2})du/v)] \quad , \tag{5}$$

$$\psi_{\mathrm{II}}(\xi)=2\pi\int_0^b \rho d\rho\{\int_{-c}^{\xi-c}dy[1-\exp(-i\int_{-c}^{y}V([\rho^2+u^2]^{1/2})du/v)] + \int_{-c}^{-\xi+c}dy[1-\exp(-i\int_y^{y+\xi}V((\rho^2+u^2)^{1/2}du/v)]+\int_{-\xi+c}^{c}dy[1-\exp(-i\int_y^c V([\rho^2+u^2]^{1/2})du/v)]\} \quad . \tag{6}$$

For $\xi \geq 2a_0$, one obtains

$$\psi(\xi)=\lim_{b\to 0}\psi_{\mathrm{I}}(\xi) \quad . \tag{7}$$

Thus, for large ξ, $\psi(\xi)$ is of the form of that of the impact approximation, $C+\sigma\xi$. This is a straight line and its slope can easily be computed to better than 1% as long as Eq. (7) is integrable. For small ξ, $\psi_{\mathrm{II}}(\xi)$ is predominant in $\psi(\xi)$ and gives the correlation function of the quasistatic approximation. In the present calculation, where rd is intermediate in magnitude, the values of $\psi(\xi)$ in the intermediate region of ξ are important, and both $\psi_{\mathrm{I}}(\xi)$ and $\psi_{\mathrm{II}}(\xi)$ must be calculated.

As a procedure of the calculation, the slope σ for the linear region of $\psi(\xi)$ is first found from Eq. (7) for $a_0\to\infty$. The calculation of the constant term of Eq. (7) is time consuming, so that the constant is found by evaluating $\psi(\xi)$ of Eq. (3) from small ξ up to the value of ξ, where $d\psi(\xi)/d\xi$ is equal to σ within a few percent, and then extrapolating the slope at the end to $\xi=0$. Here, the fact that $\psi(\xi)$ oscillates for small ξ should not be overlooked. A rough estimate of the point where $\psi(\xi)$ for small ξ is made to continue to $\psi(\xi)$ for large ξ is made from the relation $\xi\sim 2a_0$, assuming a_0 to be a so-called optical collision diameter. This procedure of continuation is, in practice, required since the integration of Eq. (3) takes too much computer time for large ξ.

The difference potential, assumed here, is

$$\hbar V(R)=\hbar\left(\frac{\alpha}{R^{12}}-\frac{\beta}{R^6}\right) \quad , \tag{8}$$

where α and β are estimated [from Mahan's calculated values[5] of the van der Waals's constants and the position of the red satellite, 32 cm^{-1}, $\mathrm{Cs}(1)/\mathrm{Xe}(^2P_{3/2})^3$] as:

$$\alpha = 1.4864\times10^{-74}\ \mathrm{cm}^{12}\ \mathrm{sec}^{-1}\ ,$$
$$\beta = 6.896\times10^{-31}\ \mathrm{cm}^{6}\ \mathrm{sec}^{-1}\ , \tag{9}$$

in angular units. In a similar calculation with a square-well potential, the position of the red satellite shifts toward the unshifted position of the line with temperature, so that the depth of the potential minimum of Eq. (8) is adjusted to be 25% larger than the observed position of the satellite. The value of β is less than Mahan's value by 14%. The reason is that the observed half-width of the $^2P_{3/2}$ component of Cs(1) perturbed by Xe at a low ω_0 seems to be slightly smaller than expected from Mahan's value. The reason for the small value is not clearly known.

In performing the integration of Eq. (3), it is rewritten

$$\psi(\xi) = 2\pi\int_0^\infty R^2dR\int_{-1}^{1}dx \times\left[1-\exp\left(-i\int_0^\xi V([R^2+2x\eta R+\eta^2]^{1/2})\frac{d\eta}{v}\right)\right]. \tag{10}$$

Introducing Eq. (8) into Eq. (10), the integrand is expanded for large R and small R compared with ξ and integrated. The exponential function in Eq. (10) is an oscillating function with ξ and slowly changes with x except for $x\sim-1$, where the exponent diverges. However, this divergence difficulty can be eliminated by the fact that when such divergence takes place the oscillation is very rapid and the oscillating part of the integrand has no contribution to the integral.

For the intermediate region of R, a numerical integration of Eq. (10) is performed on a computer. The increment of R in the integration is adjusted such that the argument of the exponential function in Eq. (10) increases by about 0.3 for every R increment. The argument of the exponential function is expanded and integrated (over η) for large and small ξ/R compared with 1. For the intermediate region of ξ/R it is formally integrated and simplified before the numerical integration in order to minimize any error involved in subtracting, on a computer, two numbers of nearly equal magnitude, except for the case when $x\sim-1$.

RESULTS AND DISCUSSION

The calculated result of $\psi(\tau)$ for large τ is, in units of cm^3, for $T=666\ ^\circ\mathrm{K}$, expressing τ in sec,

$$\psi(\tau) = (0.155-0.296i)\times10^{-20} + (0.228-0.156i)\times10^{-8}\tau\ , \tag{11}$$

and for $T=800\ ^\circ\mathrm{K}$,

$$\psi(\tau) = (0.186-0.258i)\times10^{-20} + (0.241-0.176i)\times10^{-8}\tau\ . \tag{12}$$

$\psi(\tau)$ for small τ is depicted in Fig. 1. The continuation of the calculated slopes of $\psi(\tau)$ for large and small τ is made at around $\tau=2\times10^{-12}$ sec. Within the accuracy of Fig. 1, $\psi(\tau)$ is the same for the two different temperatures for 3×10^{-12} sec $>\tau>4\times10^{-14}$ sec (the largest difference in this region is about 3%). For $\tau<4\times10^{-14}$ sec, the discrepancy in $\psi(\tau)$ for the two temperatures becomes more obvious, and the red (and the violet) satellite is more intense for the higher temperature, as seen in Fig. 2. In Fig. 1, a correlation function for a square-well difference potential of radius 6 Å and of depth $5\times10^{12}\ \mathrm{sec}^{-1}$ (angular frequency) when the relative velocity is 4.5×10^4 cm/sec, corresponding to $T=666\ ^\circ\mathrm{K}$ of the present case, is given for comparison. A definite large oscillation extends to a large τ in the square-well potential case, giving a resolved strong red satellite at $-23\ \mathrm{cm}^{-1}$ away from the unshifted line.

Figure 2 shows the calculated line profiles at

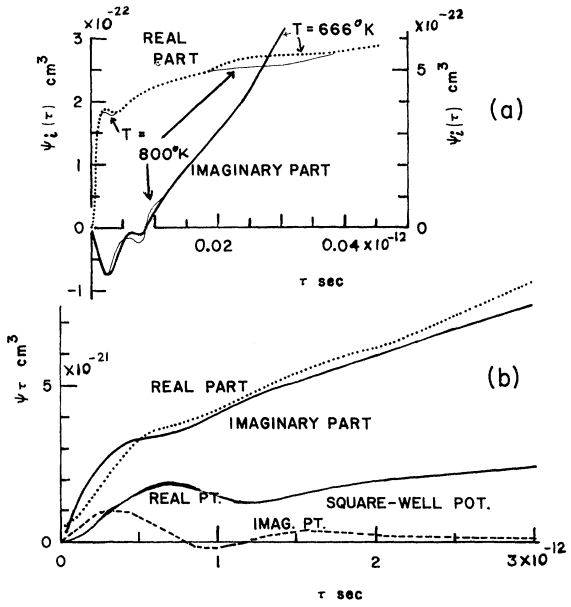

FIG. 1. $\psi(\tau)$ for $T=666$ and 800 °K. (a) for τ from 0 to 0.03×10^{-12} sec, and (b) for τ from 0.03×10^{-12} to 3×10^{-12} sec. In either case, the sign of $\psi_i(\tau)$ has been changed.

rd = 10 for T = 666 and 800 °K, and at rd = 16 for T = 666 °K. For comparison, an experimentally observed line shape[7] obtained at rd = 11.4 and T = 418 °K is given. Since the temperatures are quite different, these profiles cannot be compared exactly, but it is interesting to note that the calculated profile at rd = 10 agrees very well with the observed one at the violet shoulder, within the experimental error, justifying partly the assumptions made at the beginning. Following the definition of a satellite, the separation of the satellite is made from the calculated total line shapes at rd = 10 and they are depicted in the same figure. It can be seen that the red satellites are too weak to let the total line shape agree with the observed one at the red shoulder. When rd = 16, the calculated profile agrees fairly well with the observed one at the red shoulder, except for the exact position of the red satellite peak, but then totally disagrees in other regions. The observed peak intensity of the violet satellites[7] is about 4.4% of the total line peak intensity at rd = 11.4, while the calculated one is about 0.7% of the total line peak intensity at rd = 10. This discrepancy may be considered to be due to the fact that in the calculated line shape the red satellite, because it is weak, has not developed enough at the expense of the line intensity, so that the line is unreasonably strong, thus making the peak intensity ratio smaller compared with the observed one. However, this is not the case. In fact, at rd = 40, when the red satellite has developed strongly, either in the observation or in the calculation (the line intensity in the sense of the definition of a satellite becomes very small), the observed ratio of the violet satellite peak intensity to the total line peak intensity is about 0.33,[7] while the calculated one is 0.06. Even though the calculated ratio increases with rd a little faster than the observed one, the discrepancy is still large at a high rd. Thus, this calculation shows clearly that the violet satellites are much too weak compared with the observed one.

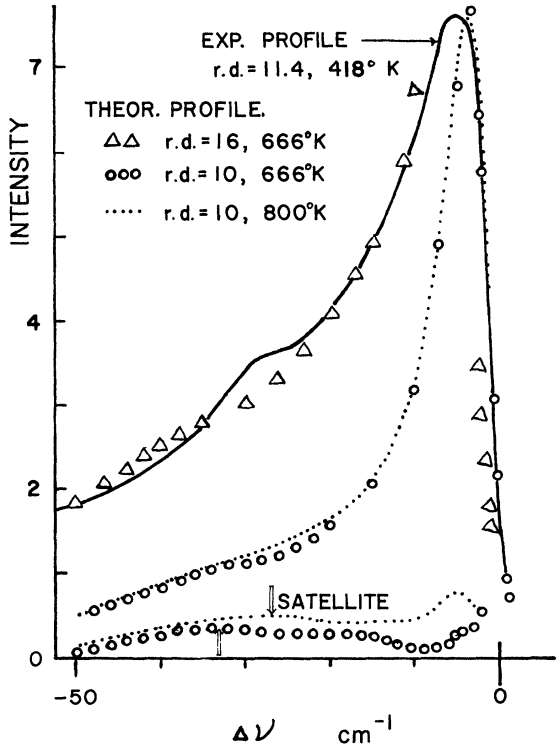

FIG. 2. Comparison of an experimentally observed total line profile (rd = 11.4, T = 418 °K) (Ref. 7) and theoretical total line profiles at rd = 10 (T = 666 and 800 °K) and at rd = 16 (666 °K). For rd = 10, separated satellites are also given.

The artificial choice of the values α and β and temperature might have caused the above discrepancy, but this is not likely. The larger line broadening due to higher temperature does not lead to the agreement of the calculated line profiles and the observed one at the red shoulder. In addition, it is confirmed that, even though the value of β is not artificially modified so that $\alpha = 2.07\times10^{-74}$ cm^{12} sec^{-1} and $\beta = 7.86\times10^{-31}$ cm^6 sec^{-1} and at T = 387 °K, the correlation function is very similar to that of Fig. 1 even for very small τ, hardly giving the satellites of observed intensity. Further, the difference potential for the $^2P_{3/2}$ component of Rb(1)/Xe[9] has a similar value for α and β givin in Eq. (9), if it is approximated by a Lennard-Jones potential, but the observed red satellite intensity is much higher than the calculated one. This indicates that the Lennard-Jones potential is inadequate for a line shape calculation under the present approximation. Assuming that the theoretical van der Waals's constants used are fairly accurate, it might require that the potential includes at least the R^{-8} term to make the well wide. The well in the difference potential should not be so deep because the red satellite is rather close to the unshifted line. This requires the repulsive part to start to be effective at a larger R. However, a calculation has not been made by introducing the additional terms to the difference potential.

Figure 3 shows the total line profiles and satellites at rd = 10, 20, and 40 calculated with the values of α and β of Eq. (9) for T = 800 °K. The red satellite grows with rd and the total line shape at rd = 40 is predominantly the shape of the satellite at the rd. The slight hump seen on the violet shoulder at rd = 40 is due to the pressure modification of the two

sharp peaks seen for rd = 10. In order to show that this hump is a real one, an experimental line profile obtained at rd = 34.5 and $T = 444$ °K is also given. The discrepancy between the experimentally observed and calculated line profile at the red shoulder is probably due to the appearance of the second satellite (strong in the experiment but weak in the calculation) expected at such a high rd. In addition to the calculated two sharp peaks, there are two violet satellites at rd = 10, which make a shift toward the unshifted line with rd rather slowly compared with the red shift of the total line peak. Two violet satellites are experimentally observed and their rd behavior agree very well with the observation.[7]

Figure 4 shows the shift, half-width, and asymmetry of the $^2P_{3/2}$ component of Cs (1)/Xe as a function of the rd of Xe. The discrepancy of their rd behavior from those observed may be simply due to the too-small intensity of the calculated red satellite. For comparison, Fig. 5 shows the shift, half-width, and asymmetry of a line broadened when the difference potential is of a square-well type of depth 5×10^{12} sec^{-1} and radius 6 Å, and the relative velocity is 10^5 cm/sec. In this case, the line carries an unresolved red satellite. All the qualitative features of the experimental line shape behavior are seen in the figure, including small oscillations about the average behavior of the half-width. Such oscillations have been in magnitude within experimental errors.[1]

Thus, the over-all behavior of the calculated line profile agrees qualitatively with the observed one, but the agreement is only in the sense of trend. The main discrepancy in the quantitative behaviors seems to be due to the satellites which are too weak in the calculated line profile because of the inadequacy of the Lennard-Jones potential

The author wishes to express his gratitude to Professor S.Y. Ch'en for his constant encouragement and financial support.

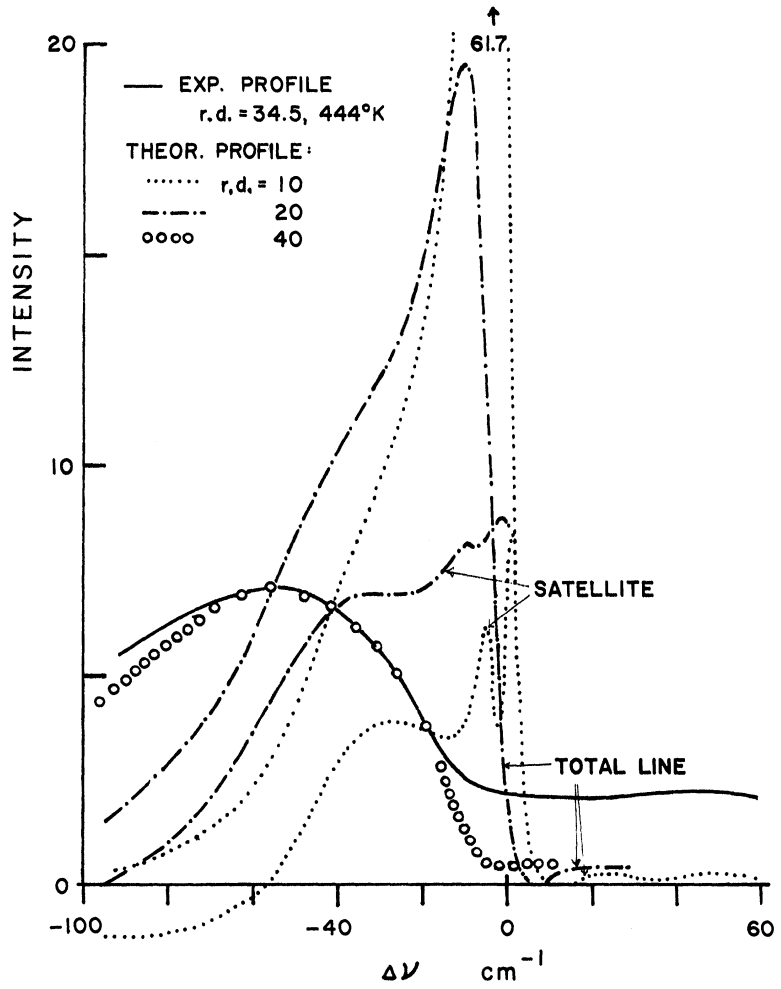

FIG. 3. Total line profiles and separated satellites at $T = 800$ °K for rd = 10, 20, and 40. An experimentally observed profile (rd = 34.6, $T = 444$ °K) is also shown for comparison (Ref. 7).

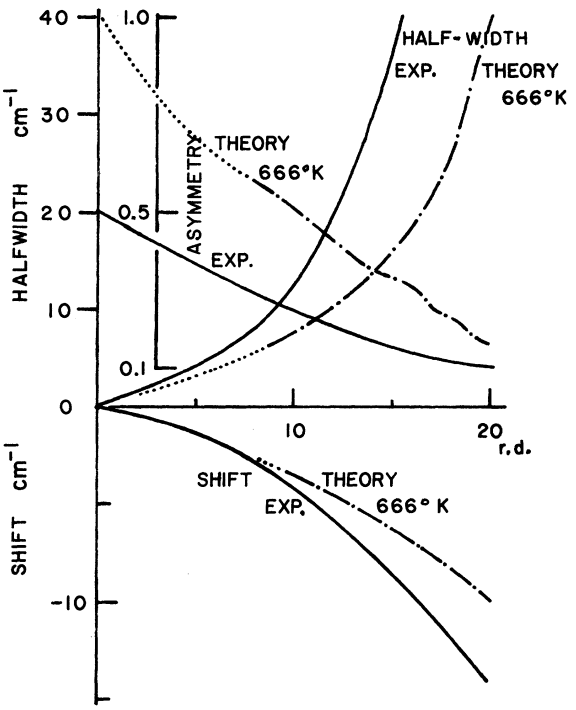

FIG. 4. Shift, half-width, and asymmetry as a function of rd. Experimental curves are obtained at $T=310$ to 440 °K (Ref. 7). For the dotted part of the theoretical curves, the assumptions used are doubtful.

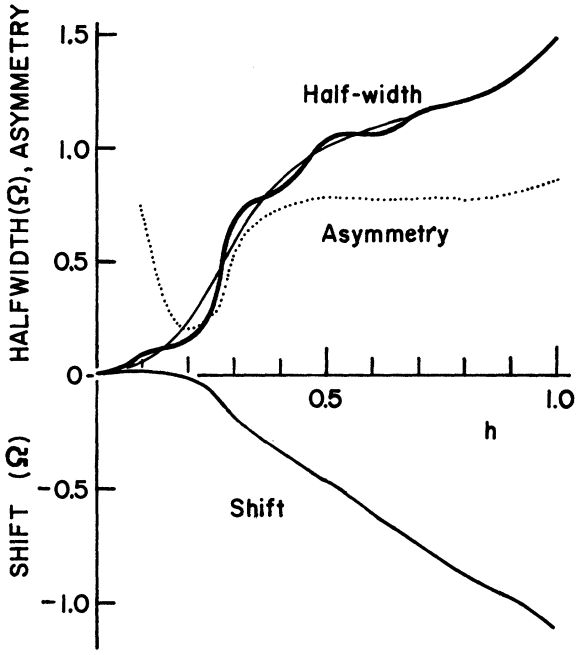

FIG. 5. Shift, half-width, and asymmetry as a function of rd for a square-well potential of depth 5×10^{12} sec^{-1} and radius 6 Å and a relative velocity of 10^5 cm/sec. Ω is in units of 8.4 cm^{-1}, and h is the average number of perturbers in the well.

*Supported by the National Science Foundation, GP-9280, and the Air Force Office of Scientific Research, Office of Aerospace Research, U.S. Air Force, under AFOSR Grant No. AF-AFOSR-1220-67.

†On sabbatical leave at University of Oregon from Portland State University.

[1]S. Y. Ch'en and R. O. Garrett, Phys. Rev. 144, 59 (1966); 144, 66 (1966); S. Y. Ch'en, E. C. Looi, and R. O. Garrett, *ibid.* 155, 38 (1967); 156, 48 (1967); S. Y. Ch'en, D. E. Gilbert, and D. K. L. Tan, *ibid.* 184, 51 (1969).

[2]E. Czuchaj and J. Fiutak, Bull. Acad. Polon. Sci. 14, 647 (1966); and (unpublished); W. Behmenberg, Z. Astrophys. 69, 368 (1968); B. Bezzerides, Phys. Rev. 181, 379 (1969); D. D. Hearn and P. R. Fontana, J. Chem. Phys. 51, 1871 (1969); D. Robert, M. Giraud, and L. Galatry, *ibid.* 51, 1871 (1969).

[3]S. Y. Ch'en and M. Takeo, Rev. Mod. Phys. 29, 20 (1957).

[4]W. Behmenberg, J. Quant. Spectry. Radiative Transfer 4, 177 (1964); W. R. Hindmarsch, A. D. Petford, and G. Smith, Proc. Roy. Soc. (London) A297, 296 (1967); J. M. Vaughan and G. Smith, Phys. Rev. 166, 17 (1968); J. Kieffer, J. Chem. Phys. 51, 1852 (1969).

[5]G. D. Mahan, J. Chem. Phys. 50, 2755 (1969).

[6]L. Klein and H. Margenau, J. Chem. Phys. 30, 1556 (1959); H. Margenau and H. J. Jacobsen, J. Quant. Spectry. Radiative Transfer 3, 35 (1963).

[7]D. E. Gilbert and S. Y. Ch'en, Phys. Rev. 188, 40 (1969).

[8]P. W. Anderson and J. D. Talman, Proceedings of the Conference on Broadening of Spectral Lines, 1956 (unpublished), p. 29; Bell Telephone System, Technical Publication No. 3117, 1956 (unpublished).

[9]S. Y. Ch'en and C. W. Fountain, J. Quant. Spectry. Radiative Transfer 4, 323 (1964).